

Development of Edible Packaging Material from Mango (*Mangifera Indica*) Seed Using RSM Software

Dr. HemaPrabha.P

Associate Professor

Department of Food Processing and Preservation Technology

Avinashilingam Institute of Home Science and Higher Education for Women

Coimbatore

Hemaprabha_fppt@avinuty.ac.in

Ms. Gokulpriya.R

Department Of Food Processing and Preservation Technology

Avinashilingam Institute of Home Science and Higher Education for Women

Coimbatore

20032uef14@avinuty.ac.in

Ms. Kanishka.K

Department Of Food Processing and Preservation Technology

Avinashilingam Institute of Home Science and Higher Education for Women

Coimbatore

20046uef19@avinuty.ac.in

Ms. Shenbaga Preetha.R

Department Of Food Processing and Preservation Technology

Avinashilingam Institute of Home Science and Higher Education for Women

Coimbatore

20097uef39@avinuty.ac.in

Abstract

The escalating environmental concerns associated with the widespread usage of non-biodegradable plastics in food packaging have spurred the need for innovative and sustainable alternatives. This delves into the development of a groundbreaking solution by harnessing the untapped potential of mango seeds to create edible packaging materials. Mango seeds, often overlooked and discarded as a waste, emerge as a valuable resource due to their unique combination of beneficial nutrients and film forming properties. The primary objective of this study is to explore the viability of mango seed-based films as a green alternative of traditional non-biodegradable packaging materials. The methodology involves the extraction of powder from mango seeds, followed by the formulation and optimization of edible films using response

surface methodology by Box-Behnken design. Through a systematic approach, the study investigates the influence of various parameters on film properties to optimal results. The critical aspect of this review is through evaluation of the physical, mechanical and barrier properties of the developed mango seed-based films. The results indicate promising characteristics, showcasing the potential of mango seed-based films to serve as an environmental and nutritious alternative to conventional packaging materials.

Keywords – Bio-degradable, Edible packaging, Film casting, Food preservation, Mango seed.

1. Introduction

Mango (*Mangifera indica* L.) is grown worldwide and widely accepted by consumers for its sweet taste and exotic flavor. During consumption and processing of mango, a large quantity of by-products in the form of peel and seeds are generated and generally discarded as waste. Mango waste generated at domestic and industrial levels requires [1] attention and proper solution for its disposal and value addition. In recent past, mango seed kernels have received a great attention, considering their nutritional and pharmaceutical importance [2]. Mango seeds contain a significant number of proteins, fats, carbohydrates, and some specific bioactive compounds. The mango seed kernel contains 53.34 to 76.81% carbohydrates, 5.20 to 10.48% proteins, 9.84 to 18.0% fat/oil, and 0.26 to 10.60% crude fiber. Specifically, mango seed kernel is a remarkable source of phytochemicals having the potential to improve human health and prevent the growth of pathogenic microorganisms. Mango seed kernel possesses phytosterols, carotenoids, tocopherol, polyphenols (*Mangifera*, hesperidin, vanillin, penta-o-galloyl-glucoside, rutin, quercetin, kaempferol, etc.), and phenolic acids (gallic acid, caffeic acid, ellagic acid, ferulic acid, etc.). These phytochemicals are known for their high antioxidant, anticancer, antimicrobial, antidiabetic, and antiplatelet aggregation properties. Phytochemicals present in mango seed kernel showed antimicrobial activity against *Staphylococcus aureus*, *Escherichia coli*, *Vibrio vulnificus*, *Candida albicans* and *Xanthomonas campestris*. This systematic review summarized the nutritional and bioactive compounds of mango seed kernel used in the development of edible packaging material which offers a viable alternative to conventional packaging materials, addressing current environmental challenges while ensuring the safety and quality of food products.

2. Materials and Methods

2.1 Raw Materials and Equipment's

The mango seed powder was prepared by the drying of mango seeds followed by washing with water, grinding and sieving process. The mango seed powder was analyzed for moisture content, protein, fat, ash content and starch content. Glycerin and gelatin were procured from the stores, Coimbatore.

2.2 Preparation of Edible Films

Mango seed powder, Glycerin, Gelatin of varying proportions were used for the film formulation by solvent casting method [3]. The filmogenic solution was prepared using the dispersing of mango powder and the addition of glycerin and gelatin in the distilled water and stirring in a magnetic stirrer at 800 rpm for 1-2 hrs. at room temperature. Petri plates were filled with 15ml of solution for casting the film and dried for 24 hrs at 40°C [4].

2.3 Chemical Properties

2.3.1 Moisture Content

The moisture content was determined using a hot air oven set at 105°C for eight hours, the moisture content of film samples was determined using three distinct combinations of constituent proportions (Zhang, 2011). The following formula was used to determine the moisture content:

$$MC (\%) = (M_1 - M_0)/(M_1) \times 100 \quad (1)$$

where M₁ is the initial weight of the film and M₀ is the final weight of the film respectively. The moisture content for the three film samples of each formulation was determined and the average value was recorded.

2.3.2 Solubility

A 2 cm diameter film sample was weighed, placed in a beaker with 50 ml of distilled water, and sealed. This beaker was kept at 25°C for 24 hours while being gently shook every now and then. Once a consistent weight was attained at 40°C, the samples were dried in a vacuum oven (Prakash maran. J, 2013). The following formula was used to determine the sample's total soluble matter:

$$Sol (\%) = (M_0 - M_1)/(M_1) \times 100 \quad (2)$$

where M₀ and M₁ were the dry sample weight before and after the test, respectively. The tests were performed thrice and the average value was calculated.

2.4. Mechanical Properties

2.4.1. Tensile Tests

Tensile strength is the ability of a material to withstand a pulling (tensile) force. It is measured in units of force per cross sectional area. The maximum amount of tensile stress that it can take before failures, such as breaking or permanent deformation is defined as the tensile strength of a material. A Universal tensile strength tester was used to test the tensile properties of the film samples [5]. The film samples of each composition of size 100 mm×15 mm was taken. A Micrometer is used to measure the thickness of the film samples at 10 arbitrary points and the average of these values was taken to calculate the cross-sectional area (equal to thickness multiplied by width) of each sample. The samples were held tightly between pneumatic clamps. The ends of each specimen were mounted using a utility tape to prevent and cracking of films during testing. Force (N) and deformation (mm) were recorded during extension at 40 mm min⁻¹ by maintaining a uniform grip separation rate. Triplicate samples of each film were tested. Experiments were run within 3 min of removing films from desiccators to minimize adsorption/desorption of water by films. Tensile strength (MPa) and Elongation at break (%) were the parameters that were determined and calculated.

2.4.2. Thickness

The dried film thicknesses are measured with an electronic digital micrometer that has been calibrated to within ±1 mm. Thirty films were randomly assessed for thickness at various points, and the mean values of each film were expressed in millimeters (mm). (Shahavi, Muhammad Hassan1, 2015).

2.4.3. Swelling capacity

Triplicate film samples of size 30 mm ×10 mm was dried to a constant weight (initial weight - M₀) by using a vacuum oven at 40°C. The dried films were immersed in 50 ml distilled water in a beaker. The beakers were sealed and kept at 25 ° C for 24 h. The drying of samples was taken place in a vacuum oven to a constant weight (final weight M₁) at 40°C. Swelling capacity was calculated and the average was taken for the samples [6]

$$Swelling (\%) = (M_1 - M_0)/(M_0) \times 100 \quad (3)$$

where M₀ is the initial weight of the sample and M₁ is the weight of swelled sample, respectively.

2.5 Barrier Properties

2.5.1. Water Vapor Transmission Rate (WVTR)

The Water Vapor Transmission Rate WVTR of biodegradable films was calculated by using Mocon Permatran, according to the standard of ASTM 2000. A modified test cell was used containing 15ml of distilled water to immerse the film. This test cell was then kept in a desiccator containing pre-dehydrated silica gel [7]. The whole assembly was kept for the weight loss of the test cell was measured after storage for 24h at 25°C. WVTR of the film was calculated according to the equation,

$$\Delta W / (\Delta t \times A) \tag{4}$$

Where ΔW is the weight loss of test cell, Δt is the time of storage and A is the area of the exposed film, respectively. The tests were carried out ambient conditions at 25°C and the determination of average of the mean values were calculated by repeating the tests for three +times and were calculated.

2.5.2. Oxygen Transmission Rate (OTR)

Using the OXTRAN Oxygen Permeability Tester at 23 °C and 0% relative humidity at 1 atm, the oxygen transmission rate (OTR) of biodegradable films was determined in accordance with ASTM D3985 standards. The average value was computed after three measurements were made at various locations throughout the film (Zhang, Effects of surfactants on the functional and structural aspects of kuduz starch or ascorbic acid films, 2011). The environmental conditions were used to condition each sample. The following formula can be used to calculate the oxygen permeability:

Oxygen permeability = OTR/ (Film thickness) (mm)*O₂ Partial pressure.

2.4. Experimental analysis and statistical analysis

Table 1. Experimental range and levels of independent variables

Variables	Coded Variables	Variable levels	Step change value ▲ Zi
		-1 0 1	
Mango seed powder(w/w)	X1	3 4 5	1
Glycerol (w/v)	X2	0.3 0.6 0.3	0.3
Distilled water(w/v)	X3	0.1 0.2 0.1	0.1

Using Response Surface Methodology (RSM) and the statistical program Design Expert 8.0.7.1 from Stat-ease Inc., Minneapolis, USA, experimental design and statistical analysis were carried out to investigate the impact of various independent parameters on all dependent variables [8]. Because it necessities fewer runs than a central composite design (CCD) in situations involving three or four variables, the Box-Behnken experimental design (BBD) was chosen especially for this purpose [9].

When compared to a three-level full-factorial design, the Box-Behnken spherical, rotating response surface methodological design provides sufficient solutions and reduces the number of tests needed, which becomes increasingly important as the number of factors increases [10]. As stated in Table 1, each independent variable was coded at three levels, ranging from +1 to -1. The relationships between coded and actual values are represented by the following equation for statistical computation:

$$X_i = (Z_i - Z_{cp}) / \Delta Z_i \tag{5}$$

where X_i was an independent variable's dimensionless value. The real value of an independent variable was denoted by Z_i , the step change of the real value of the variable i corresponding to a variation of a unit for the dimensionless value of the variable i , and the real value of an independent variable at the center point was represented by Z_{cp} . Design Expert 8.0.7.1, Stat-ease Inc., Minneapolis, USA is a statistical program that was utilized to find the pertinent model that correlated the responses with the independent variables [11]. The BBD was fitted with a second-order polynomial model, from which a quadratic model which also contains the linear model was generated.

$$Y = \beta_0 + \sum_{i=1}^k \beta_i X_i + \sum_{j=1}^k \beta_{jj} X_j^2 + \sum_{i < j} \beta_{ij} X_i X_j \tag{6}$$

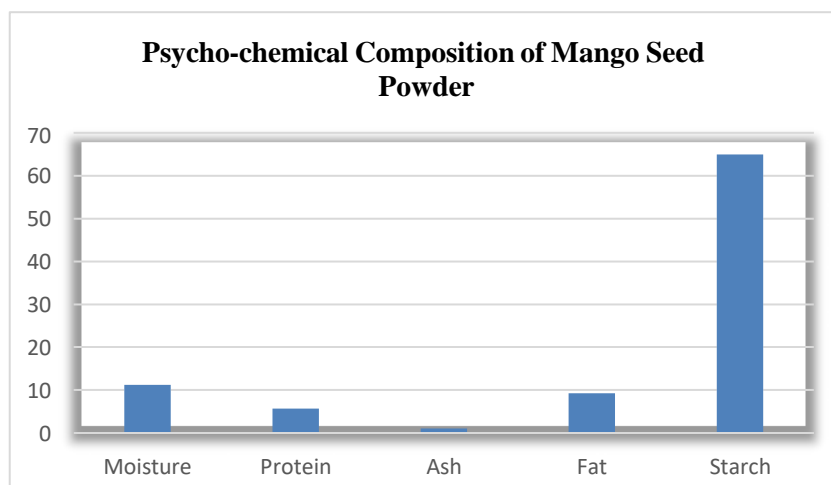
where X_i and X_j are variables (i and j range from 1 to k); β_0 is the model intercept coefficient; β_j , β_{jj} , and β_{ij} are the interaction coefficients of linear, quadratic, and second-order terms, respectively; k is the number of independent parameters ($k=3$ in this study); and e_i is the error [12]. Using the Pareto analysis of variance (ANOVA) approach, the models' adequacies were assessed. The models' adjusted- R^2 values and coefficient of determination (R^2) were also assessed. Based on the variables for each response, the F and R^2 values were calculated. Regression coefficients were utilized as a function of the variables on each answer to do statistical calculations that produced 3-D surface plots and contour plots by changing two parameters while holding the other two constant (each at its center level). Table 2 shows the physical and chemical makeup of mango seed powder. Moisture (%), Protein (%), Ash (%), Fat (%), Starch (%). A statistical analysis technique called response surface methodology (RSM) uses quantitative data from a suitable experimental design to pinpoint the ideal conditions. Statistical analysis was Moisture (11.2%), Protein (5.7%) Ash (1.1%), Fat (9.3%), Starch (65%).

Table 2. Psycho-Chemical Composition of Mango Seed Powder

Moisture %	Protein%	Ash%	Fat%	Starch (%)
11.2	5.7	1.1	9.3	65

For each constituent, triplicate samples were used to calculate the mean values and standard deviations.

Figure 1: Psycho-chemical Composition of Mango Seed Powder



3. Result and Discussion

3.1 Physio-chemical composition of Mango seed powder

The composition of mango seed powder is presented in Table 2[13]. The chemical analysis revealed that the Mango seed powder contained Moisture content (11.2%), Protein content (5.7%), Ash content (1.1%), Fat content (9.3%) and Starch content (65%) respectively as given in Table 2 and depicted in Fig. 1 [13]. The Moisture content in the mango seed powder contributes to the film forming properties and the Starch complexes that are formed during the casting process is responsible for the film forming capacity [14].

3.2 Box-Behnken analysis

Experiments were performed according to the Box Behnken experimental design where, a total number of 6 experimental trials including five center points were carried out and the experimental results are shown in Table 3 [15]. The study was carried out to relate the individual [5] and the interaction between the three independent variables (Mango seed powder, Glycerol and Distilled water) on the barrier qualities (Tensile strength and Water absorption capacity) of the biodegradable films made of Mango seed powder. In general, unless the model shows a strong fit, exploration of a fitted response surface may yield subpar or deceptive findings, which is why it is crucial to verify the model's suitability [16]. In order to derive the regression equations, the acquired data is fitted into linear, interactive, quadratic, and cubic models. As a result, response surfaces and models for each response are produced [17].

Table 3. Experimental design and responses of the dependent variables (Trials)

Run	Mango seed powder (gm)	Glycerol (ml)	Distilled water (ml)	Tensile Strength (MPa)	Water absorption capacity (gm/m ²)
1	3	15	100	16.56	40
2	3.5	25	100	14.6	43
3	3.5	17.5	75	15.6	42
4	5	25	100	17.02	45
5	3.5	10	50	17.9	40
6	2	10	75	18.6	42
7	3.5	25	50	17.6	45
8	2	25	75	14.6	42
9	3.5	10	100	14.9	46
10	2	25	50	15.6	42
11	5	17.5	50	15.69	43
12	2	17.5	100	15.89	40
13	5	17.5	100	12.6	41
14	3.5	17.5	75	18.9	42
15	5	25	75	16.98	46
16	3.5	17.5	75	18.6	45
17	5	10	75	19.2	45

TABLE 4. Sequential model of sum of squares

Source	Sum of squares	do	Mean Square	f-value	p-value	
Mean vs Total	4639.48	1	4639.48			
Linear vs Mean	13.04	3	4.35	1.41	0.2849	Suggested
2FI vs Linear	5.20	3	1.73	0.4958	0.6933	
Quadratic vs 2FI	9.33	3	3.11	0.8497	0.5094	
Cubic vs Quadratic	18.95	5	3.79	1.14	0.5290	Aliased
Residual	6.66	2	3.33			
Total	4692.65	17	276.04			

Response 1: Tensile Strength

Table 5. Sequential Model Of Sum Of Squares

Source	Sum of squares	df	Mean Square	f-value	p-value	
Mean vs Total	31175.53	1	31175.53			
Linear vs Mean	19.05	3	6.35	1.55	0.2499	
2FI vs Linear	10.28	3	3.43	0.7948	0.5243	
Quadratic vs 2FI	25.51	3	8.50	3.38	0.0837	Suggested
Cubic vs Quadratic	8.96	5	1.79	0.4134	0.8158	Aliased
Residual	8.67	2	4.33			
Total	31248.00	17	1838.12			

Response 2: Water Absorptiveness

Table 6. Fit Statistics

Std.Dev.	1.59	R²	0.7568
Mean	42.82	Adjusted R²	0.4441
C.V.%	3.71	Predicted R²	0.0721
		Adeq Precision	6.1067

Table 7. Model Summary Statics Tested For Tensile Strength

Source	Sequential p-value	Lack of Fit p-value	Adjusted R ²	Predicted R ²	
Linear	0.2849	0.6314	0.0711	-0.2892	Suggested
2FI	0.6933	0.5709	-0.0512	-1.2295	
Quadratic	0.5094	0.5290	-0.1009	-2.7527	
Cubic	0.5290		-0.0020		Aliased

TABLE 8. Model summary statics tested for Water Absorptiveness

Source	Sequential p-value	Lack of Fit p-value	Adjusted R ²	Predicted R ²	
Linear	0.2499	0.6223	0.0928	-0.2560	
2FI	0.5243	0.5923	0.0477	-1.7470	
Quadratic	0.0837	0.8158	0.04441	-0.0721	Suggested
Cubic	0.8158		0.0433		Aliased

3.3 RSM model fitting

In order to fit the projected values into the quadratic model, statistical significance must be tested using ANOVA analysis (analysis of variance) [18]. Analysis of variance (ANOVA) was used to examine the statistical significance of the ratio of mean square variation owing to regression and mean square residual error. In order to test hypotheses regarding the model's parameters, ANOVA is a statistical technique that splits the overall variance in a set of data into component components linked to certain sources of variation [19]. The coefficient of determination, linear significance, lack of fit, and interaction effects are all computed using the analysis of variance [20]. The suitability and sufficiency of the created models with respect to response variables and process factors were also examined as per the table [8] [21]. The outline of the reciprocal and mutual interactions between the process variables was revealed by using the probability value (p-value) to examine each coefficient's importance. A p-value less than 0.05 suggests that the model is statistically significant, and a p-value more than 0.05 implies that the associated coefficient has a greater degree of significance [22]. The ratio of sum of squares due to regression (SSR) to total sum of squares (SST) is indicated by the coefficient of determination (R²), which indicates the percentage of the overall variation in the response predicted by the model. A reasonable agreement with modified R² is required, and a high R² value, near to 1, is preferred [23]. The statistical significance of the quadratic model is demonstrated by its p-value, which is less than 0.0001. According to the model summary statistics, the cubic model was found to be aliased in WVTR and OTR, while the quadratic

model had the highest "Adjusted R-Squared" and "Predicted R-Squared" values. ANOVA As an appendix to Table 7, Table 6 demonstrated a perfect fit of the quadratic regression model with F-values of 103.3767, p b 0.0001 for WVTR and F-value of 59.31808, p b 0.0001 for OTR, respectively. For WVTR, the "Adj R-Squared" of 0.880519 and the "Pred R-Squared" of 0.982931 are reasonably in accord. For OTR, the "Adj R-Squared" of 0.992923 and the "Pred R-Squared" of 0.970418 are reasonably in accord in table 5. Table 6 makes clear that the quadratic model was suggestive and demonstrated strong fit for both responses, whereas the cubic model was found to be aliased. Based on the Box-Behnken experimental design, a second-order polynomial equation was created for the answers, as shown in Table 3. The experiment's outcomes and the process variables were used to fit the equation. The highest order polynomial where the additional terms are significant and the model is not aliased is predicted in Table 4. The coefficient estimate represents the expected change in the response per unit change in the factor value when all remaining factors are held constant. The intercept in an orthogonal design is the overall response of the all runs. The coefficients are adjustments around that average based on the factor settings. When the factors are orthogonal the VIF's are 1; VIF'S greater than 1 indicates that multi collinearity, the higher the VIF the more severe the correlation of factors. As a rough rule, VIFs less than 10 are tolerable. A negative Predicted R² implies that the overall mean may be a better predictor of your response than the current model. In some cases, a higher order model may also predicted better. Adeq Precision measures the signal to noise ratio. A ratio greater than 4 is desirable. The ratio of 6.107 indicates an adequate signal. This model can be used to navigate the design space.

Table 9. coefficient In Terms of Coded Factors

Factor	Coefficient Estimate	df	Standard Error	95% CI Low	95% CI High	VIF
Intercept	42.21	1	0.8793	40.13	44.29	
A-Manqo Seed Powder	1.89	1	0.5825	0.5117	3.27	1.22
B-Glycerol	0.6278	1	0.5374	-0.6430	1.90	1.14
C-Distilled Water	0.4918	1	0.5624	-0.8381	1.82	1.23
AB	0.3993	1	0.7194	-1.30	2.10	1.24
AC	-0.6915	1	0.8090	-2.60	1.22	1.32
BC	-1.67	1	0.7102	-3.35	0.0101	1.22
A ²	-0.6561	1	0.8083	-2.57	1.26	1.07
B ²	2.54	1	0.8918	0.4324	4.65	1.26
C ²	-1.27	1	0.8022	-3.17	0.6280	1.05

Table 10. Anova And Significance of Regression Coefficients

Source	Sum of Squares	df	Mean Square	F-value	p-value	
Model	54.85	9	6.09	2.42	0.1285	not significant
A-Mango Seed Powder	26.48	1	26.48	10.52	0.0142	
B-Glycerol	3.44	1	3.44	1.36	0.2810	
C-Distilled Water	1.93	1	1.93	0.7646	0.4109	
AB	0.7755	1	0.7755	0.3080	0.5962	
AC	1.84	1	1.84	0.7306	0.4210	
BC	13.91	1	13.91	5.52	0.0511	
A ²	1.66	1	1.66	0.6589	0.4437	
B ²	20.44	1	20.44	8.12	0.0247	
C ²	6.30	1	6.30	2.50	0.1577	
Residual	17.62	7	2.52			
Lack of Fit	8.96	5	1.79	0.4134	0.8158	not significant
Pure Error	8.67	2	4.33			
Cor Total	72.47	16				

3.3.1 Contour and Three-Dimensional Response Surface Plots

To see the relationship between the response and process variables, contour plots were made. and to investigate the relationships between response tensile strength and water absorptiveness, a three-dimensional response surface was created. Figure 2 illustrates that the two-dimensional circular contour plot of residues and the three-dimensional response surfaces, which revealed mutual interactions between the response and process variables and a linear correlation. Figure 3 illustrates that the three-dimensional response surface which revealed that comparison between predicted and experimented values. To determine the optimal processed settings, the responses were analysed using design expert software. To determine the ideal circumstances for both dependent and independent variables, second order polynomial models were created for each answer. Figs. 4 and 5 show the box- cox plots of the studentized residuals and the cook’s distance of tensile strength and water absorptiveness.

Figure 2: Normal plot of residues

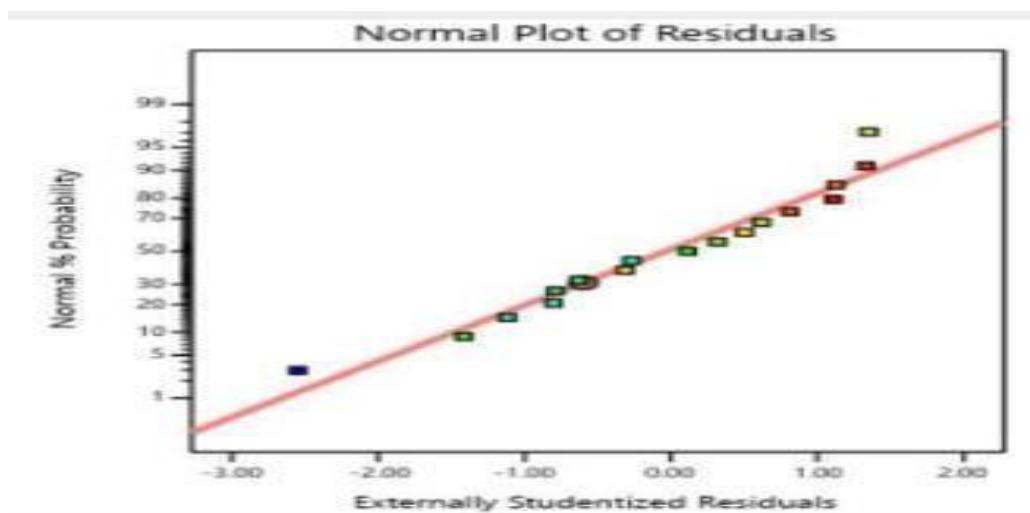


Figure 3: Comparison between predicted and experimental values

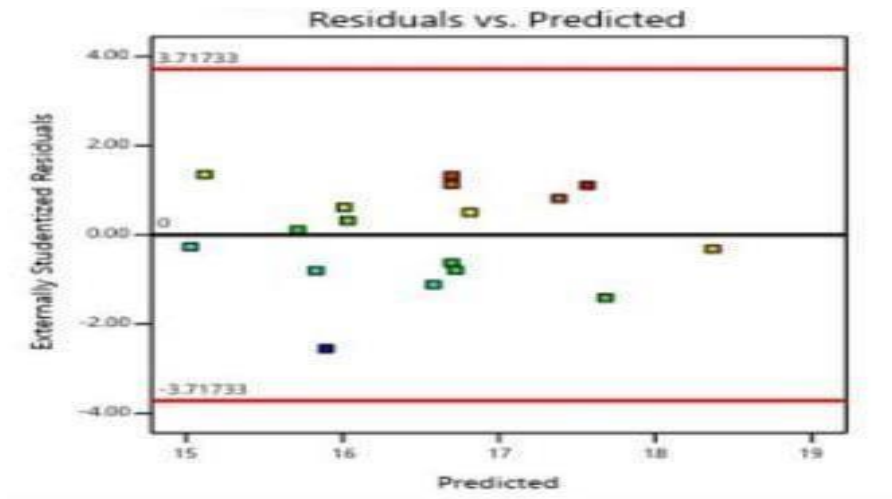


Figure 4: Box-Cox plot for power transforms

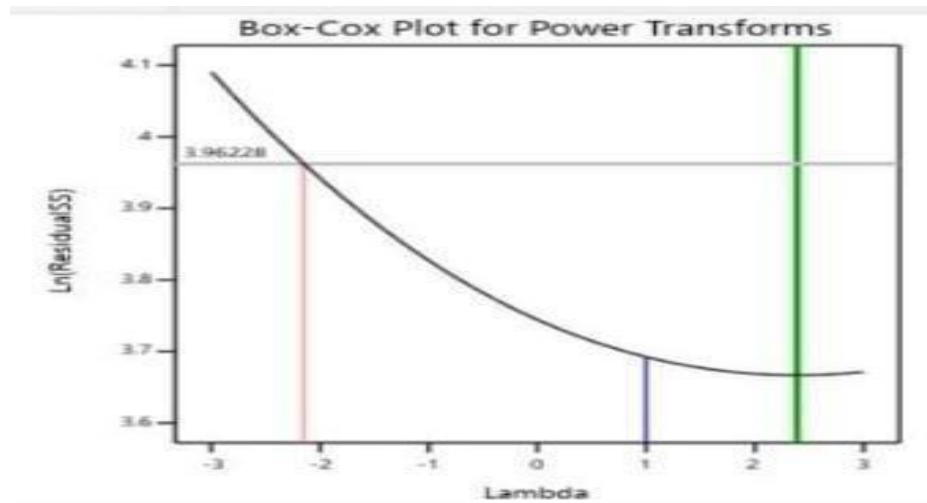
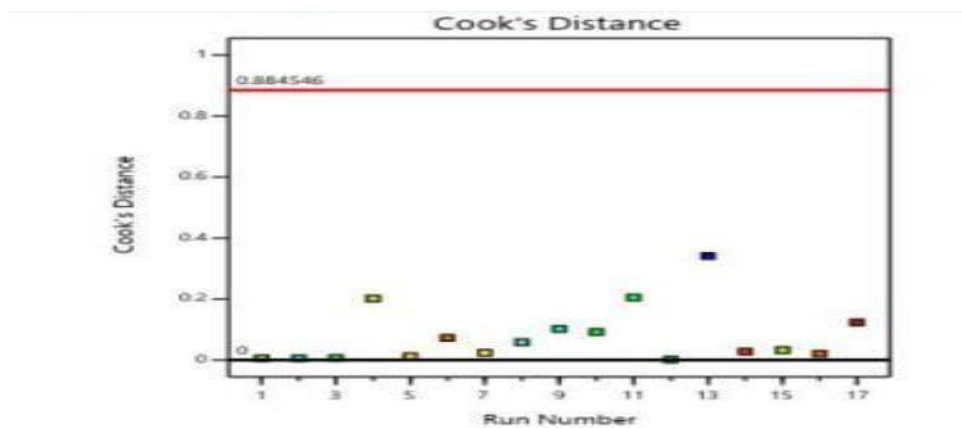


Figure 5: Cooks distance



3.3.2 Effect of Process Variables and Validation of Optimized Condition

To determine the optimal processed settings, the responses were analysed using design expert software. For every response, second order polynomial models were created in order to determine the ideal circumstances for both the dependent and independent variables. The contour plot for Tensile Strength and Water absorption capacity under ideal conditions, as indicated in Table 3, shows how the trials were carried out. The statistical program Design Expert 8.0.7.1, produced by Stat-ease Inc., Minneapolis, USA, was used to evaluate the validation data [24]. Table 3 makes clear that the presence of Mango seed powder, Glycerol and Distilled water affected the Water absorption capacity. One of the most crucial aspects of film is its ability to absorb water, as this significantly boosts the film's usefulness in the food industry [25]. As the films develop thicker, more water molecules attach themselves to the polar groups inside the matrix because starch is hydrophilic [26] [27]. Eventually, less water vapor seeps through the films as a result of this. It should be mentioned that the film provides a greater resistance to mass transfer across it as its thickness increases [28].

Figure 6: Response surface plot (3-D) showing the interaction effect of process variables on Tensile Strength

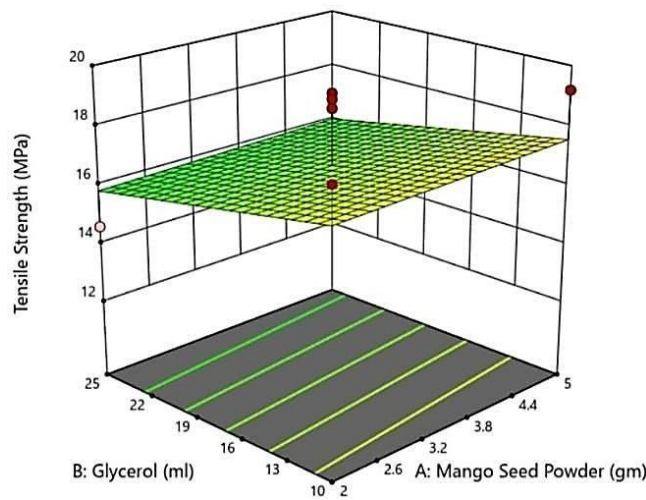
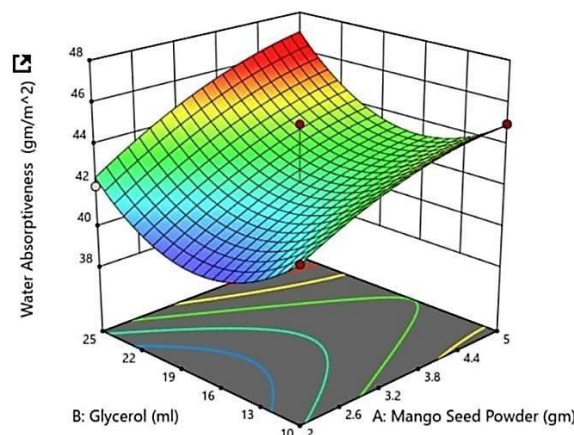


Figure 7: Response surface plot (3-D) showing the interaction effect of process variables on Water Absorption Capacity.



Changes in starch and glycerol levels and variations in film thickness are caused by pore development, which allows water vapor to permeate. The water vapor transfer rate is accelerated by the intermolecular bonding that occurs between the glycerol molecules and the starch polymer chain [29]. The hydrophilic effect of mango seed powder and glycerol increases the film's tensile strength, while a decrease in the concentration of glycerol and distilled water causes an interconnecting polymeric network to form, increasing the film's tensile strength. Table 3 makes it clear that the process factors had a major impact on the tensile strength. The response plots of tensile strength and water absorption capacity showed that all three process factors significantly influenced all response variables, either independently or interactively, once the optimal levels of the process parameters were reached [30]. The obtained findings clearly demonstrate that the appropriateness of the created quadratic models within the ideal levels of the process parameters, the optimal values of quadratic models are valid.

3.4 Nutrition Information

Sl.No	Name Of The Test	Result	Test Method
1.	Energy	273 Kcal	FSSAI Manual of methods
2.	Total Fat	0.5gm/100gm	FSSAI Manual of methods
3.	Carbohydrate	62.4gm/100gm	FSSAI Manual of methods
4.	Protein	4.6gm/100gm	FSSAI Manual of methods
5.	Vitamin B12	15mcg/100gm	FSSAI Manual of methods

3.5 Antioxidant

Sl. No	Name Of the Test	Result	Test Method
1.	Total Antioxidant Capacity	60µg/ g ascorbic acid	By UV-VIS spectrophotometric method

4. Conclusion

By optimizing the process variables Mango seed powder, glycerol and distilled water, response surface methods with Box-Behnken experimental design were used to explore the physical, mechanical, and barrier qualities biodegradable films. High-quality protein with all necessary amino acids can be found in mango seeds. Mango seed oil is devoid of trans fats and high in unsaturated fatty acids. The food business has a lot of possibilities for using mango seeds. In order to assess the importance of the process factors on the film's qualities, response surface plots were created. To describe the relationship between the process variables and the response variables, mathematical models containing second-order polynomials were created using the experimental data for each response variable. It was discovered that the two most important factors ($p < 0.05$) affecting the response variables were cassava starch and glycerol. The findings show that when starch and glycerol levels grew, so did the MC and S of the starch films; However, the concentrations of starch, plasticizer, and solubilizer primarily regulate the various qualities of the film. The findings showed that using Box-Behnken response surface design to create efficient bio-based packaging films for food packaging applications might yield the ideal amounts of process variables.

5. References

- [1] A. R. H. M. C. S. L. M. M. Kehinde Ganiyat Lawal, "Development of Carboxymethylcellulose Based Active and Edible Food Packaging Films Using Date Seed Components as Reinforcing Agent: Physical, Biological, and Mechanical Properties," *Food Biophysics*, pp. 1-13, 2023.
- [2] T. B. D. T. C. K. S. P. K. Poonam Choudary, "Mnago seed kernel: A bountiful source of nutritional and bioactive compounds," *Food and Bioprocess Technology* 16(2), pp. 289-312, 2023.
- [3] Arlington, "AOAC," *Official methods of analysis of Aoac International*, 1995.
- [4] C. C.E.Chinma, "Chemical composition, functional and pasting properties of tapioca starch and soy protein concentrate blends," *J.Food Sci.Technol.*, p. 50(6), 2013.
- [5] A. a. A. Bonilla.J, "Properties of wheat starch film-forming dispersion and films as affected by chitosan addition," *J.Food.Engg,114:*, pp. 303-410, 1995.
- [6] G. J. C. a. G. Hu, p. 291–298, 2009.
- [7] P. B. C. B. R. S. Suppakul, "Empirical modelling of moisture absorption characteristics and mechanical and barrier properties of starch and the relation to plasticizing effects," *LWT – Food Science and technology* 50:, p. 290–297, 2013.
- [8] S.-E. Inc, "Design expert software, Version 8.0.7.1," *minneapolis, USA*, 2011.
- [9] J.J.Borkowski, "Spherical prediction variation properties of central composite and Box-behnken designs," *Technometrics*, vol. 37, pp. 399-410, 1995.
- [10] D. G.E.Box, "Some new three level designs for the study of quantitative variables," *Technometrics*, vol. 37, pp. 455-477, 1960.
- [11] B. W. V. K. S. D. C. White, "Identifying and estimating significant geological parameters with experimental design," *SPE J.6*, pp. 311-324, 2001.
- [12] S. M. J.P. Maran, "Response surface modeling and optimization of process parameters for aqueous extraction of pigments from prickly pear (*Opuntia ficus-indica*) fruit," *Dyes Pigments* , vol. 95(3), pp. 465-472, 2012.
- [13] E. P. P. D. L. A. C.F. Chivrac, "Starch base nano-biocomposites: plasticizer impact on the montmorillonite exfoliation process," *Carbohydr. Polym.*, vol. 79, pp. 941-947, 2010.
- [14] L. F. A. R. S. G. L. G. S. Flores, "Physical properties of tapioca-starch edible films: influence of filmmaking and potassium sorbate," *Food Res. Int*, vol. 40, pp. 257-265, 2007.
- [15] C. A. J. A. C.E. Chinma, "Chemical composition, functional and pasting properties of tapioca starch and soy protein concentrate blends.," *J. Food Sci. Technol*, vol. 50 (6), p. 1179–1185, 2013.
- [16] F. S. C.M. Liyana-Pathirana, "Optimization of extraction of phenolic compounds from wheat using response surface methodology," *Food Chem*, vol. 93, pp. 47-56, 2005.
- [17] Y. L. Y. Zhang, "Effects of surfactants on the functional and structural properties of kudzu (*Pueraria lobata*) starch/ascorbic acid films.," *Food Hydrocoll*, vol. 85, pp. 622-628, 2011.
- [18] R. B. E. F. C. D. A. C. C. T. A.C. Souza, "Tapioca starch biodegradable films: influence of glycerol and clay nanoparticles content on tensile and barrier properties and glass transition temperature.,"
- [19] Z. G. N. S. L. Y. L. Huiping, "Technologic parameter optimization of gas quenching process using response surface method," *Compt.Mater.Sci*, pp. 561-570, 2007.
- [20] T. R. S. G. A.A. Sundarraj, "Optimized extraction and characterization of pectin from jackfruit (*Artocarpus integer*) wastes using response surface methodology.," Vols. 106(698-703), 2018.
- [21] V. S. J. M. V. P. I. ., J. H. M. [26] R. Sridhar, "Treatment of pulp and paper industry effluent by electrocoagulant process," vol. 1495–1502(2), 2011.
- [22] H. A. M. I. M. Z. ., L. Mohajeri, "Statistical experiment design approach for optimizing biodegradation of weathered crude oil in coastal sediments," Vols. 101 (893-900), 2010.

- [23] V. S. K. T. R. S. J.P. Maran, "Response surface modeling and analysis of barrier and optical properties of maize starch edible films," Vols. 412-421(60), 2013.
- [24] G. M. H. A.K. Mohantya, "biofibres biodegradable polymers and biocomposites," *Macromol. Mater. Eng.*, pp. 1-24, 2000.
- [25] M. M. N. Z. M.A. García, "Microstructural characterization of plasticized starch-based films," *Starch-Starke*, vol. 52(4), pp. 118-124, 2000.
- [26] C. C.E.Chinma, "Chemical composition,functional and pasting properties of tapioca starch and soy proteins concentrate blends," *J.food Sci.Technol.*50(6).
- [27] M. G. M. G. M. M. N. Z. S. Mali, "Mechanical and thermal properties of yam starch films.," *Food Hydrocoll*, vol. 19(1), pp. 157-164, 2005.
- [28] C. N. L. R. S.K. Bajpai, "Water vapor permeation and antimicrobial properties of sago starch based films formed via microwave irradiation," *Int. Food Res. J.*, vol. 18, pp. 417-426, 2011.
- [29] B. P.Suppakul, "Empirical modelling of moisture absorption characteristics and mechanical and barrier properties of tapioca flour film and their relation to plasticizing- antiplasticizing effects," *LWT food sci-Technol*, vol. 50, pp. 290-296, 2013.
- [30] R. P. J. S. P. F. P. Myllarinen, "Effect of glycerol on behavior of amylose and amylopectin films.," *Carbohydr.Polym*, vol. 50, pp. 355-361, 2002.
- [31] Y. a. Y. L. Zhang, "Effects of surfactants on the functional and structural properties of kudzu(Pueraria lobata) starch/ascorbic acid films," *Carbohydrate polymers*, pp. 622-628, 2011.
- [32] S. b. Prakash maran.J, "Response surface modelling and analysis of barrier and optical properties of maize starch edible films," *Int.J.of Bio.Macro.*60:, pp. 412-421, 2013.
- [33] M. H. Mohammad Hassan Shahavi1, "Optimization of encapsulated clove oil particle size with biodegradable shell using design expert methodology," *Pak. J. Biotechnol.*12(2), pp. 149-160, 2015.
- [34] Y. a. Y. L. Zhang, " Effects of surfactants on the functional and structural properties of kuduz starch or ascorbic acid films," *Carbohydrate Polymers* 85:, p. : 622–628, 2011.
- [35] W. K. L. L. C.H. Chen, "Effect of surfactants on water barrier and physical properties of tapioca starch/decolorized Hsian-Tsao leaf gum films," *Food Hydrocoll*, vol. 23, pp. 714-721, 2009.
- [36] F. G. P. C. J. Y. X. M. Y. Wu, " Effect of agar on the microstructure and performance of potato starch film," *Carbohydr. Polym*, vol. 76, pp. 299-304, 2009.